Macroplastic transfer dynamics in the Loire estuary: Similarities and specificities with macrotidal estuaries

L. Ledieu, R. Tramoy, David Mabilais, Sophie Ricordel, L. Verdier, B. Tassin, Johnny Gasperi

Marine Pollution Bulletin, 182(2022)
https://doi.org/10.1016/j.marpolbul.2022.114019

Macroplastic transfer dynamics in the Loire estuary: similarities and specificities with macrotidal estuaries

L. Ledieu[1], R. Tramoy[2,3], D. Mabilais[1], S. Ricordel[1], L. Verdier[1], B. Tassin[2,3], J. Gasperi[1]

[1] Univ Gustave Eiffel, GERS-LEE, F-44344 Bouguenais, France.

lauriane.ledieu@univ-eiffel.fr; johnny.gasperi@univ-eiffel.fr

[2] Univ Paris Est Créteil, LEESU, F-94010 Créteil, France.

[3] Ecole des Ponts, LEESU, F-77455 Champs-sur-Marne, France.

Abstract

The quantification of macroplastic fluxes transferred by rivers toward the pelagic environment requires a better understanding of macrodebris transfer processes in estuarine environments. Following the strategy adopted in the Seine estuary, this study aims to characterize macroplastic trajectories in the Loire estuary. Between January 2020 and July 2021, 35 trajectories were monitored using plastic bottles equipped with GPS-trackers. With total travelled distances between 100 m and 103.6 km, trajectories show great spatiotemporal variability. The various forcing factors (macroplastic buoyancy, estuaries tidal and hydrometeorological conditions, geomorphology and vegetation) lead to chaotic trajectories, preventing accurate predictions in macroplastic transfer and storage/remobilization dynamics. In the Loire estuary like in the Seine one, no tracked bottle reached the Atlantic Ocean. It confirms that macrotidal estuaries under temperate climates constitute accumulation zones and slow pathways for macroplastics, but raises question on the real fluxes transferred from continental areas to oceans.

Keywords: Storage, remobilization, GPS, buoyancy, geomorphology

1. Introduction

The negative impact of anthropogenic litter, especially macroplastics, has been largely enounced (van Emmerik and Schwarz, 2020; Vegter et al., 2014) and become an increasing topic of interest in environmental sciences. Rivers were pointed out as major pathway for macroplastics (Bruge et al., 2018; Lechthaler et al., 2020; Schmidt et al., 2017). As estuarine environments are at the land-ocean interface, it is crucial to know how these complex systems contribute to plastic dynamics at this interface. Like for other pollutants, the challenge is to know

if estuaries constitute sink or sources (Schöneich-Argent et al., 2020; Vermeiren et al., 2016) but few studies deal with macroplastic transfer and accumulation in these environments (van Emmerik and Schwarz, 2020; Mazarrasa et al., 2019; Pinheiro et al., 2021; Tramoy et al., 2020a, b).

Within rivers, the transfer of macroplastics over short spatiotemporal scales is driven by hydrometeorological conditions namely water level, current velocity and flow (van Emmerik et al., 2020a; van Emmerik and Schwarz, 2020) as well as inherent characteristics of macroplastics like their shape, size, mass and composition, affecting their buoyancy and thus their mode of transportation (Vermeiren et al., 2016). Estuaries are actually complex systems with (i) a strong influence of wind speed and direction (Browne et al., 2010; Rech et al., 2014), (ii) the adding role of tides (Sadri and Thompson, 2014), (iii) the influence of atmospheric pressure on water levels (Tramoy et al., 2020b), and (iv) the variable hydrological conditions along the estuarine gradient (Possatto et al., 2015) with the presence of the Turbidity Maximum Zone (TMZ; Vermeiren et al., 2016). The complex interactions of these processes lead to chaotic dynamics depending on many parameters (e.g. tidal and hydrometeorological conditions, estuarine gradients). Because of this complexity, the spatiotemporal evolutions and residence time of macroplastics are difficult to quantify and remain poorly understood (Tramoy et al., 2020a; van Emmerik et al., 2022).

Meijer et al. (2021) estimated an annual amount of macroplastics entering the oceans between 0.8 and 2.7 million metric tons and González-Fernández et al. (2021) between 1 656 and 4 997 metric tons at the European scale. Estimations on the basis of statistics and conceptual models however show large discrepancies with field observations (Castro-Jiménez et al., 2019; Dris et al., 2020; González-Fernández et al., 2021). Moreover, among the few investigations of macroplastic transport and accumulation in estuarine systems, methodological dissimilarities make most of the time the results difficult to compare (Dris et al., 2020). New technologies currently developed make these applications easier. For example, remote sensing were used to draw the distribution of plastic litter from local to global scales (Duncan et al., 2020) but especially in marine environments (Biermann et al., 2020; Maximenko et al., 2019). In environments at land-ocean interfaces, Duncan et al. (2020) and Tramoy et al. (2020a) demonstrated a good capacity to follow the macroplastic transfer dynamics at short spatiotemporal scales by using GPS tracking bottles in the Ganges delta and the Seine estuary, respectively.

In the Seine estuary, Tramoy et al. (2020a, b) showed back and forth movements as well as storage/remobilization processes leading to a long residence time of macroplastics, up to decades. These results

suggest that estuarine systems mainly act as accumulation zones and thus as slow pathways releasing low amounts of plastics to the ocean. But, is this behavior general or site-specific?

This paper proposes a comprehensive approach of macroplastic transfer and accumulation dynamics along the Loire estuary. To help discussing the analogies and specificities of the Loire estuary, the same methodology than Tramoy et al. (2020b) was used by the release of bottles equipped with GPS-trackers. This study aims to (i) provide a site-specific comprehension of the fate of macroplastics within the Loire estuary for a better management of this contamination, (ii) confirm the role of tidal and hydrometeorological conditions by the monitoring trajectories between January 2020 and July 2021, (iii) assess the influence of buoyancy by the release of paired bottles: one floating and one ballasted and (iv) discuss the role of estuarine specificities in the macroplastic transfer and accumulation on the basis of two feedbacks from the Seine and the Loire estuaries.

2. Material and methods

2.1. Loire River estuary

The Loire River is 1 006 km long and drains about 20% of the French territory (Sellier, 2012; Figure 1b). Its estuary starts at Ancenis, 97 km upstream the river mouth (Figure 1c) and is the second largest of the French Atlantic coast (SNPN, 2008). At the estuary entrance, water flow ranges from around 100 m^3/s to more than 6 000 m^3/s (mean water flow equals to approximately 850 m^3/s at Montjean sur Loire; Sellier, 2012). Worldwide, different types of estuaries exist according to their tidal ranges (micro-, meso- and macrotidal, Figure 1a). With tidal ranges up to 6 m (Boët et al., 2011), the Loire estuary is qualified as macrotidal (Figure 1a). The extension of the Turbidity Maximum Zone (TMZ) is variable according to water flows and tidal ranges (GIP, 2014). TMZ extends at least until the kilometric point (pk) 15 and at most until pk 66 (GIP, 2014; Figure 1c).

In its estuarine part, the Loire River is bordered by tilted blocks constituting staggered plateaus and hillsides at low elevations. It is therefore characterized by a flat topography which appears symmetric from North to South (Figure 1c). These steps-shaped riverbanks lead to the formation of the most diverse wetlands of France (6.5% of its surface; SNPN, 2008; Figure 1c) which are managed and protected (SAGE, 2020) for their high ecological value. This is particularly the case for reedbeds, covering between 2 300 and 2 800 ha (GIP, 2016). Wetlands downstream from Nantes (Figure 1c) also constitute significant submersible areas (SAGE, 2020).

With the presence of Nantes agglomeration (sixth most populated city in France), more than 1 million of people lived in the part of the Loire watershed from Ancenis to the rivermouth (3% of the total watershed surface) in 2016 (SAGE, 2020). Nevertheless, along the estuary, the landcover is mainly composed of agricultural lands (Figure 1c). Because of the port activities of St-Nazaire and Nantes, the Loire estuary has undergone many modifications: channeling, containment, enrockment as well as the construction of hydraulic (e.g. herringbones) and navigation structures (Sellier, 2012). As a result, the Loire estuary is slightly meandered (sinuosity index of 1.1) contrary to the Seine River (sinuosity index of 1.9). Moreover, the estuary flares towards the river mouth, passing from a width of 200 m upstream, to about 15 km at the river mouth (Sellier, 2012; Figure 1c).

2.2. Tracker program and data collection

To perform the monitoring, the same customized tracked bottles than Tramoy et al. (2020b) were used. It consists of 1 L plastic bottles, commonly used for water sampling and made of HDPE, equipped with GPS-trackers (©INETIS). In order to ensure waterproof conditions and a good transmission, very compact GPS-trackers were chosen to be easily placed in the bottles without playing a key role in their buoyancy. The INET-OS operating system of these GPS-trackers is configurable, which makes possible to set a tracker program adapted for this study. Moreover, the GPS-tracker contains accelerometers enabling to save battery energy through a standby mode. In a perspective of reproducibility, the tracker program defined by Tramoy et al. (2020b) was used, program available on request. The program uses grafcet language and was programmed with three states: “state 0” when the tracker is off, “state 1” when the program starts after motion detection or clock setting, and “state 2” when the program is on standby after 14 h without motion. During state 1, the tracker records one position every 2 h to get several positions during a tidal cycle (12 h) for 33 trajectories. Moreover, 2 trajectories were recorded with a higher temporal resolution, i.e. one position every 30 min. State 2 aims to save battery energy during stranding episodes longer than one tidal cycle. However, the program goes back to state 1 when the tracker detects motion again. Recorded positions were sent once a day to a server with a GSM/GPRS system.

2.3. Experiment design

Except for the influence of bottle’s buoyancy, it was chosen to adopt a stochastic approach to observe bottles trajectories, i.e. by the release of bottles at different locations of the estuary and during different conditions

of water flow and tidal range, and to describe them through a Lagrangian description. Between January 2020 and July 2021, 35 trajectories were therefore monitored in the Loire estuary (Table S1). The locations of release are mapped in Figure 1c and detailed characteristics of each location are in Table S1: 10 were released upstream Nantes in the estuarine-fluvial zone of the estuary and 25 were released in the internal estuary, including 19 in Nantes urban area and 6 downstream. To avoid a quick stranding on riverbanks, 46% of the bottles were released in the middle of the channel from bridges (Table S1). The remaining 54% were thrown in the river from riverbanks, approximately 5 m from the riverbank (Table S1). All details about initial and final conditions of the tracked bottles are available in Table S1. References and information relative to the tracking experiment were tagged on bottles to enhance possibilities of recovery. Nevertheless, among the 35 bottles released, 6 were definitively lost either because of the loss of the signal (n = 3), or by accidental picking of a cleanup service (n = 1), or because they were stuck under navigation structures (n = 2; Table S1). Their trajectories were however considered because the program used enables to recover sent positions on the server.

The influence of bottles buoyancy was observed through the release of two 1L-bottles at the same time and same place (57% of the trajectories, Table S1): one empty, i.e. floating, and one ballasted with sand, i.e. half-submerged. “Empty bottles” had a mass ranging from 169 to 250 g (density 0.161 to 0.238, Table S1) resulting in high buoyancy, lying on the water surface (16 to 24 % of the volume submerged, Table S1) and letting a significant surface area subjected to wind. They are called “floating bottles”. In contrast, the ballasted bottles had a mass ranging from 790 to 1 004 g (density 0.752 to 0.956, Table S1). They stayed vertical (75 to 96 % of the volume submerged, Table S1) and are called “half-submerged bottles”. In this case, the GPS-tracker was maintained in the emerged part of the bottle with expanded foam.

2.4. Data treatment

A trajectory represents the course of a tracked bottle in space and time between its release and its retrieval (or loss). It therefore includes the water transport and the stranding episodes. The following parameters were recorded: initial and final conditions, distances, speeds, stranding/remobilization episodes, and tidal and hydrometeorological conditions (Table 1). Water flow data were taken at the Montjean-sur-Loire station (Figure 1b) on http://www.hydro.eaufrance.fr/ and water levels, flood/ebb tides and tidal ranges were taken at the St-Nazaire station on http://maree.info/. The trajectories were rebuilt using GPS positions processed by QGIS (QGIS.org, 2022). To calculate distances and speeds, kilometric points (pk) were assigned to each GPS position.

These points are calculated along a virtual streamline in the middle of the channel positively oriented upstream. In this study, pk 0 was set at St-Nazaire (Figure 1c). The characteristics of the stranding sites (i.e. riverbank and vegetation typologies) were also reported under QGIS using the data supplied by the GIP Loire Estuaire.

Statistical tests were performed to rank the influence of each environmental variable (site of release, water flow and tidal ranges). Statistics were performed with RStudio 1.4.1717 (RStudio Team, 2021). Respective weights of influencing factors (environmental conditions and bottles buoyancy) on trajectory parameters were assessed through a principal component analysis (PCA) using "FactoMineR" (Lê et al., 2008), "ggplot2" (Wickham, 2016) and "factoextra" (Kassambara and Mundt, 2020) packages.

3. Results

3.1. Macroplastic transfer dynamics in the Loire estuary

All parameters are described in Table 1 and written in italic in the following parts. The trajectories exhibit *total durations* ranging from 6 h to 64 days (median value equals to 11 days, Figure 2, Table S2). The tracked bottles thus spent up to two months on field. Over the 35 trajectories, 32 show to a *total duration* longer than one day. Lower *total durations* are recorded for 3 trajectories because of signal loss (T2 and T32) and accidental picking of the tracked bottle by a cleaning service (T21, Figure 2, Table S2). As the recovery of the tracked bottles was opportunistic, the *travel time* without considering the last stranding is therefore calculated to avoid any bias. This parameter varies between ½ h and 58 days (median value equals to 14 h, Table S2) excluding T2, T21 and T32. Trajectories show high spatiotemporal variabilities with *maximum speeds* ranging from 0 (immediately stranded) to 32 km/h (median value equals to 4.2 km/h, Table S2) and *total distances* ranging from 0.1 to 103.6 km (median value equals to 10.6 km, Table S2). In comparison, *net distances* are lower, ranging from -6.4 to 59 km (median value equals to 6.3 km, Figure 3, Table S2). Here, negative *net distances* mean tracked bottles were recovered upstream their initial location release. Nevertheless, not all trajectories exhibit a difference (Figure 3) as the *(Total – Net) distances* range from 0 to 92.8 km (median value equals to 0.4 km, Table S2).

The tracked bottles *travel time in water* does not exceed 4 days (median value equals to 10 h, Table S2) illustrating stranding processes occurring quite quickly. Except one (T32, bottle lost), all trajectories exhibit at least one *stranding episode* longer than 12 h (Figure 2, Table S2). Between 1 and 3 *stranding episodes* were monitored per trajectory showing remobilization processes (Figure 2, Table S2) but 54% of the trajectories exhibit only 1 *stranding episode* (Figure 2, Table S2). Consequently, for these trajectories, the *travel time* corresponds to

the *travel time in water* (Table S2) and has to be taken with caution. Among the 46% of trajectories for which remobilization processes occurred, the *stranding time* is between 10 h and 57 days (median value equals to 3 days, Table S2). The final stranding occurred during the highest *tidal range* of the monitored period for 69% of the trajectories. In total, 55 *stranding episodes* longer than a tidal cycle (12 h) and 21 *remobilization episodes* were recorded. *Remobilization episodes* occurred mostly during *flood tides* (62%). Only 52% of these episodes truly removed the bottles to transport them between 0.2 and 65.1 km downstream (median value equals to 8.4 km, Table S3). Bottles were pushed between 0.1 and 0.2 km along riverbanks (median value equals to 0.1 km, Table S3) and between 0.2 and 1.1 km farther in submersible areas (median value equals to 0.4 km, Table S3), both for 19% of these episodes. For the last 10%, bottles were pushed between 0.2 and 1.4 km farther in lateral channels (median value equals to 0.8 km, Table S3).

Considering the *riverbank and vegetation typologies*, 73% of the *stranding episodes* occurred in intertidal areas (Figure 4, Table S3). Most of the tracked bottles stranded on natural riverbanks (36%), 25% on rock embankments, 16% on urban riverbanks, 9% in submersible areas and 7% in lateral channels (Figure 4, Table S3). Moreover, 67% of the tracked bottles were retrieved in riparian vegetation in which 54% are reedbeds and 46% are other types of vegetation like meadows or woods (Figure 4, Table S3). Among the bottles stranded in the riparian vegetation in the downstream part of the estuary, the *remobilization episodes* occurred rather in meadows or woods (59%) than in reedbeds (41%, Figure 4, Table S3).

3.2. The impact of hydrological conditions

The spatiotemporal variability of the trajectories according to the initial *water flow* was observed to identify general trends and considering the influence of this factor on trajectory parameters (Figure S1). With *water flow* (Q_i) ranging from 408 to 4 080 m^3/s (Table S2), three clusters of trajectories were designed relative to the mean value (Q_i = 1 248 m^3/s during the 35 monitored trajectories): low hydrological conditions (LHC, Q_i = 595 ± 116 m^3/s, n = 17), high hydrological conditions (HHC, Q_i = 1 219 ± 237 m^3/s, n = 12) and flood conditions (Q_i = 3 161 ± 827 m^3/s, n = 6, Table S2).

The *travel time in water* is the lowest during flood events (median value equals to 0.2 days, Figure 5a, Table S4a). During these hydrological conditions, *total* and *net distances* are equal and the highest (median value equals to 13.5 km, Figure 5a, Table S4a). The *maximum speeds* reached by the tracked bottles are also three times higher during flood events (median value equals to 9.1 km/h, Table S4a) than during LHC and HHC (median

values equal to 3.3 km/h and 3.7 km/h, respectively, Figure 5a, Table S4a). During HHC, the *travel time in water* (median value equals to 0.7 days) and *net distances* travelled by the tracked bottles (median value equals to 4.7 km) are slightly higher than during LHC (median value equals to 0.4 days and 3.9 km, respectively, Figure 5a, Table S4a). An opposite trend is however observed for *total distances* (median values equal to 5.1 km and 7.8 km during HHC and LHC, respectively, Figure 5a, Table S4a), which leads to higher *(Total – Net) distances* during LHC (median value equals to 11.2 km, Figure 5a, Table S4a).

Trajectories exhibit a median value of 1 *stranding episode* (Figure 5a, Table S4a) and most of them occurred in intertidal areas (78%, 72% and 71% for flood events, HHC and LHC, respectively, Table S3) whatever the hydrological conditions. Nevertheless, the tracked bottles mostly stranded on the north *side* during flood events (67%) and on the south *side* during LHC (61%, Table S3). Moreover, more *stranding episodes* occurred on the Loire islands during flood events and HHC (22% and 28%, respectively) than during LHC (7%, Table S3). Because of embankments and enrockments, a high proportion of bottles were retrieved in Nantes agglomeration during HHC (50%) and LHC (46%) and on natural riverbanks during flood events (67%, Table S3). The percentage of bottles remobilized after stranding was slightly higher during LHC (43%) than during flood events and HHC (33% for both, Tables S2 and S4). Nevertheless, 83% of the *remobilization episodes* truly removed the bottles to transport them elsewhere during HHC whereas this proportion falls to 42% during LHC (Table S3).

3.3. The impact of macroplastic buoyancy

With ten paired bottles released with different densities (D) at the same location and at the same time, two clusters of trajectories were designed relative to bottle's *buoyancy*: floating (F, D = 0.207 ± 0.037, n = 10) and half-submerged (H-S, D = 0.831 ± 0.064, n = 10). Floating and half-submerged bottles show different trajectories (Figure 3). A video of a paired trajectory (T19 and T20) is available on the online version of this paper and illustrates these differences. Half-submerged bottles have higher *travel time in water* (median value equals to 1.2 days) than floating ones (median value equals to 0.2 days, Figure 5b, Table S4b). As a result, *total* and *net distances* travelled by floating bottles are lower (median values equal to 5.1 km and 3.2 km, respectively) than half-submerged ones (median values equal to 18.4 km and 4.7 km, respectively, Figure 5b, Table S4b), which have consequently the highest median value of *(Total – Net) distances* (equals to 6.0 km compared to 0.7 km for floating bottles, Table S4b). Exceptions are however noticed with high *(Total – Net) distances* whatever the bottle's *buoyancy*, mostly during the spring tides with the highest *tidal range* (6 m, Figure 3). Moreover, half-submerged

bottles have lower *maximum speeds* (maximum value equals to 5.8 km/h) than floating ones (maximum value equals to 9.0 km/h, Figure 5b, Table S4b).

The number of *stranding episodes* is different between floating (12 episodes in total) and half-submerged bottles (22 episodes in total, Figure 5b, Tables S2 and S4b). Floating bottles mostly stranded in intertidal areas (75%) during *ebb tides* (67%, Table S3). In contrast, half-submerged bottles stranded as much in intertidal areas (59%) than in lateral channels (18%) or in submersible areas (14%, Table S3) because these can be carried farther. Their *stranding episodes* occurred mainly during *flood tides* (73%, Table S3). These bottles exhibit 12 *remobilization episodes* but only 7 of these episodes (58%) truly removed the bottles to transport them elsewhere (Table S3). The other episodes pushed the bottles laterally on the riverbank (8%) or farther in submersible areas (17%) and in lateral channels (17%) mostly during *flood tides* (75%, Table S3). In contrast, floating bottles exhibit 2 *remobilization episodes* and both truly removed them during *ebb tides* (Table S3). No preferential accumulation zone appears between natural riverbanks, rock embankments and urban riverbanks (Table S3). Also, no trends are observed between *end sites* and/or their *vegetation typologies* (Table S3).

4. Discussion

In agreement with the few studies performed in estuaries (Swan River (Australia), Hajbane and Pattiaratchi, 2017; Paranaguá Bay (Brazil), Krelling and Turra, 2019; Pas, Miera and Asón Rivers (Spain), Mazarrasa et al., 2019; Seine River (France), Tramoy et al., 2020b), the macroplastic transfer dynamics have a high spatiotemporal variability in the Loire estuary (Figures 2 and 3). This variability can be explained by a combination of factors. For example, *start pk* and bottles *buoyancy* are not sufficient to explain the variable *net distances* travelled by the tracked bottles (Figure 3). It evidences that plastic debris have chaotic trajectories within estuaries (Tramoy et al., 2020b) compared to their horizontal downstream transport within rivers. Forcing factors are therefore hard to quantify and to rank. The multifactor character of the trajectories is illustrated by the low weight of each factor (represented by the length of their arrows) in the PCA despite that the first two axes explain around 70% of the data variance (Figure S1). Nevertheless, the factor having the highest weight on trajectory parameters is the initial *water flow* (Figure S1). Focusing on specific physical drivers can help to highlight a better picture of the dynamics of interest (Hajbane and Pattiaratchi, 2017). That's why tidal and hydrometeorological conditions, macroplastic buoyancy as well as the estuarine geomorphology are discussed separately below.

4.1. A chaotic journey for macroplastics in the Loire estuary

4.1.1. A high residence time because of tides

Tides-induced processes play a key role in macroplastic travelled *distances* and residence time (Liro et al., 2020). In this work, values of *(Total – Net) distances* evidenced back and forth movements of the tracked bottles (Figure 2), consistently with other studies (Tramoy et al., 2020b; van Emmerik et al., 2020b). These movements derive from the bidirectional flows induced by tides and considering the maximum value of this parameter (i.e. 92.8 km), macroplastics can be easily pushed back to the upstream part of the Loire estuary. Tides also generate high variations in water levels and these variations lead to storage/remobilization processes (Tramoy et al., 2020b; van Emmerik et al., 2020b). This impact is corroborated by the increasing of both the capacity of macroplastics to strand (Kurniawan and Imron, 2019a) and debris residence time with increasing tidal ranges (section 3.1.). Moreover, Vermeiren et al. (2016) conceptualized intertidal areas as a temporary sink for macroplastics and the predominance of *stranding episodes* in intertidal areas in this study (Figure 4) confirms this concept. Debris have therefore stepwise trajectories, resulting in higher residence time within estuaries than previously thought (Ivar do Sul and Costa, 2013; Tramoy et al., 2020b; van Emmerik et al., 2020b). In the Loire estuary, the latter far exceeded the water residence time, which is between 3 and 30 days (Briant et al., 2021). Even if the tracked bottles spent up to 2 months on field and travelled up to 100 km, none of them reached the Atlantic Ocean, indicating that this estuary also constitutes an accumulation zone and slow pathway for macroplastics.

4.1.2. A significant impact of hydrological conditions

Macroplastic transfer dynamics within estuaries are also driven by the hydrological flow regime (van Emmerik et al., 2019) which drives the dominant processes between tides and river outflows (Dris et al., 2020; Tramoy et al., 2020b). Results of this study actually highlight variable dominant processes according to *water flow*. During flood events, the flushing effect of river flow-dominated processes led to a fast downstream transfer of debris over long distances (*net distances* up to 59 km, Table S4a). Despite high *tidal ranges* (up to 4.6 m, Table S2), macroplastic transfer dynamics were not affected by back and forth movements because the stranding also occurred quickly (median value of *travel time in water* equals to 0.2 days, Figure 5a, Table S4a) and even quicker when flood events occurred at *flood tides*. Consequently, as suggested by Dris et al. (2020) and van Emmerik et al. (2022), these results confirm that extreme events play a key role in the macroplastic transfer distances and residence time. Apart from extreme events, in the Loire estuary, the capacity of macroplastics to be transferred

downstream was in average limited whatever the hydrological conditions (median values of *net distances* equal to 3.9 and 4.7 for LHC and HHC, Table S4a). Nevertheless, periods of low *water flows* (Q_i < 800 m^3/s) mostly exhibited a transfer driven by tidal-dominated processes and periods of high *water flows* (800 < Q_i < 2 000 m^3/s) an intermediate behavior considering the high variability both in the *net* travelled *distances* and the effects of tides (Table S4a). Resulting from the wide range of *water flow* in the Loire estuary, the shift between tidal-dominated and river flow-dominated processes therefore appeared gradual. Moreover, by driving macroplastic transfer distances, hydrological conditions regulate the distance between debris sources and accumulation zones (Duncan et al., 2020; Tramoy et al., 2020b). It is also interesting to note that in the Loire estuary, more *stranding episodes* occurred on islands during flood events and HHC (Table S3), because of their submersion. In these cases, the vegetation on islands constitute strong accumulations zones (Liro et al., 2022). For example, during two trajectories (T6 and T12), bottles stranded on the uninhabited and therefore highly vegetated La Motte island (Figure 4). High amount of macrodebris are actually accumulated there, which supports the transfer dynamics described by the tracked bottles. Furthermore, many authors observed an increase of macroplastics with increasing *water flows* (Castro-Jiménez et al., 2019; Cheung et al., 2016; Krelling and Turra, 2019; Kurniawan and Imron, 2019b). These trends can result from increasing inputs by the washup from rainwaters on land and/or from the remobilization of macroplastics accumulated in the river and/or riverbanks (Castro-Jiménez et al., 2019; Kurniawan and Imron, 2019b; van Emmerik et al., 2022). In the Loire estuary, the percentage of *remobilization episodes* was slightly higher during LHC but the remobilization appeared more efficient (i.e. to cause a subsequent transfer in the river channel) during HHC (section 3.2). Therefore, the opportunity of the stranded bottles to be remobilized not only depends on *water flow* but this parameter drives the capacity of the remobilization processes to be efficient.

4.1.3. Specific transfer and accumulation processes according to buoyancy

Macroplastics can be transferred in different ways: floating at the water surface, half-submerged in the water column or by saltation on the riverbed (van Emmerik et al., 2020a). In the Loire estuary, floating debris appeared to strand more quickly than half-submerged ones. This behavior was already noticed (Ryan and Perold, 2021; Tramoy et al., 2020b) and one assumption is a greater effect of the wind on debris transferred at the water surface (Browne et al., 2010; Maclean et al., 2021; van Emmerik and Schwarz, 2020). This is supported in the Loire estuary by higher *maximum speeds* of floating bottles than half-submerged ones (Table S4b). No correlation was observed with wind conditions but these variables are difficult to consider because of very local conditions (e.g. wind gusts). Floating debris will consequently accumulate faster and closer to their entry point in the estuary

(Maclean et al., 2021), as supported by their low *net distances* (Table S4b). In contrast, half-submerged bottles appeared more sensitive to the water current than floating bottles and can be longer transported in the water column. However, like demonstrated by their *net distances*, they travelled not necessarily higher distances by being more prone to back and forth movements with tides (Figure 3 and 5b, Table S4b). Given these dissimilarities and based on our feedback on the Loire estuary, buoyancy also affects the storage/remobilization processes. Floating bottles mostly stranded in intertidal areas whereas half-submerged bottles can be deposited farther from the river channel (Table S3). Moreover, floating bottles appeared less sensitive to remobilization processes (section 3.3.) suggesting a higher residence time than half-submerged ones once stranded. Nevertheless, half-submerged bottles were not always removed until the river channel to be reexported. On the contrary, in some cases (34%), these *remobilization episodes* pushed them farther from the main channel thanks to the estuarine geomorphology (submersible areas, plateaux at low elevation, etc.) during high *tidal ranges* (higher than 4 m, Table S2). Two trajectories actually illustrated this lateral displacement in submersible areas (T7 and T22, Table S3) and the farthest bottle was retrieved at 1.8 km from the main channel (Figure 4).

4.2. Similarities and specificities with the Seine estuary

4.2.1. Macrotidal estuaries as accumulation zone and slow pathway for macroplastics

The same methodology was used in the Seine estuary by Tramoy et al. (2020b). Whatever the estuary geomorphology (highly and slightly meandered for the Seine and the Loire estuaries, respectively), both surveys demonstrated chaotic transfer dynamics animated by back and forth movements of the tracked bottles and by storage/remobilization processes. As demonstrated by Tramoy et al. (2020a, b), these factors increase the residence time of macroplastics which can tremendously delay their transfer to the ocean. That rivers act as “plastic reservoirs” was recently conceptualized (Tramoy et al., 2020a; van Emmerik et al., 2022) and a macroplastic accumulation was also noticed in deltaic systems (Acha et al., 2003; Duncan et al., 2020). Ryan and Perold (2021) already evoked site-specific transfer distances of macroplastics, mostly resulting from the variable impact of floods and tides in estuaries. Such processes are therefore not specific but appear enhanced in macrotidal estuaries considering their water flow-tides relation and their spring and neap tidal cycles. Only 40% of tracked bottles actually stranded in the Ganga delta (Duncan et al., 2020) whereas no bottles reached the sea during the monitoring period neither for the Loire nor the Seine estuaries. In the Seine estuary, Tramoy et al. (2020a) estimated a potential residence time up to decades. In the Loire one, the residence time could not be estimated but is in any case longer

than two months. It strengthens the recent suggestion that macrotidal estuarine systems under temperate climates mainly act as accumulation zones and slow pathways for macroplastics and that model estimations calculating the rates of plastic debris released into the oceans must consider this point (Dris et al., 2020; Tramoy et al., 2020b). It also highlights the need to focus on extreme hydrometerological events, which are most likely to remobilize the accumulated macrodebris (van Emmerik et al., 2022).

4.2.2. Site-specific dynamics according to estuarine geomorphology

Tracked bottles exhibit different trajectories in both estuaries. Experimental conditions were also variable. More trajectories were actually monitored during periods of high flows (HHC and floods, n=26) compared to low flows (LHC, n=13) in the Seine estuary (Tramoy et al., 2020b) and similar proportions of trajectories were monitored during the other hydrological conditions (LHC, n=17 and HHC and floods, n=18) in the Loire one. For a better comparison between both estuaries, trajectory parameters were therefore compared for each period (Figure 6). Regarding bottle's *buoyancy*, experimental conditions were less variable. Similar proportions of half-submerged bottles were actually released during periods of high flows (HHC and floods) in both estuaries (56% in the Loire estuary, 54% in the Seine one) and quite more in the Loire estuary (53%) than in the Seine one (39%) during LHC. The Loire estuary is shorter (i.e. 97 km), lowly meandered (sinuosity index of 1.1), and with higher *water flows* (mean Qi = 850 m^3/s) than the Seine one (i.e. 175 km, sinuosity index of 1.9 and mean Qi = 487 m^3/s; Tramoy et al., 2020b) offering a better opportunity for macroplastics to be transferred downstream. Despite a monitoring on similar time scales, the *travel time in water* was however higher in the Seine estuary than in the Loire one whatever the hydrological conditions (Figure 6, Table S5). It leads to *total and net distances* travelled by the tracked bottles mostly higher in the Seine estuary than in the Loire one even when compared in relation to the total estuarine length (Figure 6, Table S5). Therefore, even if meanders are known to enable a greater macroplastic accumulation than linear river sections (Mazarrasa et al., 2019; van Emmerik et al., 2019), the higher meandering morphology of the Seine estuary (Tramoy et al., 2020b) does not necessarily mean a quick stranding of macroplastics, or at least a high residence time once stranded. In fact, the trajectories recorded in the Seine estuary exhibited a higher number of *stranding episodes* than the Loire one (Figure 6, Table S5), suggesting that remobilization processes occur easily and more frequently. These different dynamics can be related to the difference of riverbank typologies between both estuaries. Liro et al. (2020) actually hypothesized that rivers with more diverse morphologies (wider channel, floodplain zones, islands and lateral channels) and riparian vegetations (case of the Loire River) could limit the downstream transport of macroplastics compared to channelized and embanked rivers (case of the Seine River). Results of this study illustrate this hypothesis and confirm that the

geomorphology of the Loire estuary limit the transfer of the tracked bottles which are accumulated in areas where they are difficult to remove (submersible areas, islands, lateral channels, etc.).

4.2.3. Site-specific accumulation zones according to estuarine geomorphology

Estuarine geomorphology is a predominant factor for creating macroplastic accumulation areas. Firstly, features like riverbanks with gentle slope (Browne et al., 2010; Bruge et al., 2018; Cordeiro and Costa, 2010), meanders (Mazarrasa et al., 2019; Tramoy et al., 2020b) or high and flat areas (Ivar do Sul et al., 2014) were recognized as preferential areas for accumulating macroplastics. The gentle slope as well as the presence of islands and large submersible areas tend to favor the macroplastics retention in the Loire estuary, whereas the Seine natural riverbanks are steeper. Secondly, large riparian vegetation also constitutes great accumulation zones according to literature (e.g. Bruge et al., 2018; Gonçalves et al., 2020; Ivar do Sul et al., 2014; Weideman et al., 2020; Williams and Simmons, 1997) and the Loire estuary is no exception. The trapping capacity of vegetation is driven by its structural characteristics (Mazarrasa et al., 2019) such as their height, plant density and spatial configuration (van Emmerik et al., 2022). A significant retention capacity for reedbeds has already been suggested (van Emmerik and Schwarz, 2020). The great storage of macroplastics in reedbeds in the downstream part of the Loire estuary (Figure 4; GIP, 2016) confirm this suggestion. This is also demonstrated by the low proportions of *remobilization episodes* for the bottles stranded in this type of riparian vegetation (Figure 4, Table S3). The short length of the Loire estuary actually enables the macroplastics to reach faster these strong accumulation zones. Accumulation zones can therefore show a large variability according to the estuaries considered (Rech et al., 2014). Most of the time, accumulation zones are very localized (Ryan and Perold, 2021) and site-specific investigations thus provide useful insights to locally optimize plastic recovery strategies (van Calcar and van Emmerik, 2019). In the Seine estuary for example, the Villequier site is known to strongly accumulate macroplastics and is regularly cleaned up as well as other accumulation zones (Tramoy et al., 2021). In the Loire estuary, accumulation zones appeared more diverse but some areas downstream from Nantes agglomeration and reedbeds were identified as significant ones (Figure 4). Regular clean up actions similarly to those realized in the Seine estuary could therefore be planned. If not, it can either be supposed that seasonal changes in the riparian vegetation may provoke the release of the accumulated debris or that these may be degraded into microplastics (Dris et al., 2020; Gonçalves et al., 2020; Ivar do Sul et al., 2014) creating a source of secondary microplastic within the riverine and marine ecosystems.

5. Concluding remarks, outlooks and recommendations

Macroplastic transfer dynamics show a high spatiotemporal variability within estuaries making it difficult to qualify, quantify and therefore to predict. Nevertheless, we have to improve our understanding of macroplastics evolution for a better management of this contamination and this study provides valuable information on their transfer and accumulation dynamics within an estuary at short temporal scale. Consistently with other studies on estuaries, this study illustrates that tides lead to chaotic and stepwise macroplastic transfer dynamics animated by back and forth movements and storage/remobilization processes. Such processes appear not specific but enhanced in macrotidal estuaries where tidal ranges are the highest. On the 74 tracked bottles released either in the Seine or in the Loire estuaries, none reached the ocean during their active tracking (up to two months), suggesting estuaries constitute slow pathways or even a long-lasting macroplastic reservoir. Those results raise questions about the real amount of macroplastics entering into the ocean when compared to model estimations. The enhanced downstream transport under flooding conditions balanced by enhanced storage/remobilization processes also highlights the key role of extreme events like flood events, all the more so with the ongoing climate change.

This study also corroborates that macroplastic buoyancy significantly influences their transfer dynamics and therefore their accumulation zones and residence time whatever the type of estuary considered. However, whatever their buoyancy, the macroplastic transport in macrotidal estuaries may be tidal-dominated under regular hydrological conditions, whereas it may be driven by river flow-dominated processes during high water discharge (i.e. flood events) strengthening again the need to focus on extreme hydrometeorological events. These trends appear however valid for macrotidal estuaries under temperate climates but more studies are required to confirm this hypothesis. The latter carried with comparable data and on different type of estuaries could be highly valuable. By choosing a stochastic approach to observe macroplastic transfer dynamics, we assume that only general trends can be concluded from the results. A precise assessment of the influence of tidal range, water flows and the different parts of the estuary (estuarine-fluviale zone, internal and external parts) requires a deterministic approach in the sample design like it was done for bottle's buoyancy. Nevertheless, the consideration of such variables needs a careful thought as their spatiotemporal variability are difficult to integrate. For example, the clustering designed relative to the water flow considered the water flow at start time and do not include all variations during trajectories. The difficulty is the same to evaluate the influence of wind gusts on floating macroplastic dynamics.

Moreover, intertidal areas and riparian vegetations are major actors of macroplastic retention and large accumulation zones have been identified in both estuaries. Nevertheless, given the specific geomorphology of the Loire estuary with large submersible areas, the presence of reedbeds, islands and lateral channels, it appears as a more efficient sink for macroplastics than the Seine one. Accumulation zones were actually more diverse and

widely distributed, sometimes far from the river channel. Such site-specific studies provide also important information for a better adaptation of our macroplastic removal strategies. Among the accumulation zones identified through this work, some will be subject to a monitoring while cleaning actions are already led on some others.

Acknowledgments

This work, was funded by Région des Pays de la Loire (France) and by Nantes Métropole within the framework of the Plasti-nium Research project. This project benefit from the scientific structuration of the Sciences of the Universe Observatory of Nantes (OSUNA) and its program "Grande Zone Estuarienne et Risques" (GZER). The authors gratefully thank the GIP Loire Estuaire for providing geographical data layer on the Loire estuary.

References

Acha, E.M., Mianzan, H.W., Iribarne, O., Gagliardini, D.A., Lasta, C., Daleo, P., 2003. The role of the Río de la Plata bottom salinity front in accumulating debris. Marine Pollution Bulletin 46, 197–202. https://doi.org/10.1016/S0025-326X(02)00356-9

Biermann, L., Clewley, D., Martinez-Vicente, V., Topouzelis, K., 2020. Finding Plastic Patches in Coastal Waters using Optical Satellite Data. Scientific Reports 10, 5364. https://doi.org/10.1038/s41598-020-62298-z

Boët, P., Bocquené, G., Bouleau, G., Etchebert, H., Foussard, V., Just, A., Lepage, M., Lobry, J., Moussard, S., Sirost, O., Sottolichio, A., Leveque, C., 2011. Synthèse du projet BEEST. Rapport de l'IRSTEA.

Briant, N., Chiffoleau, J.-F., Knoery, J., Araújo, D.F., Ponzevera, E., Crochet, S., Thomas, B., Brach-Papa, C., 2021. Seasonal trace metal distribution, partition and fluxes in the temperate macrotidal Loire Estuary (France). Estuarine, Coastal and Shelf Science 262, 107616. https://doi.org/10.1016/j.ecss.2021.107616

Browne, M.A., Galloway, T.S., Thompson, R.C., 2010. Spatial Patterns of Plastic Debris along Estuarine Shorelines. Environmental Science & Technology 44, 3404–3409. https://doi.org/10.1021/es903784e

Bruge, A., Barreau, C., Carlot, J., Collin, H., Moreno, C., Maison, P., 2018. Monitoring Litter Inputs from the Adour River (Southwest France) to the Marine Environment. Journal of Marine Science and Engineering 6, 24. https://doi.org/10.3390/jmse6010024

Castro-Jiménez, J., González-Fernández, D., Fornier, M., Schmidt, N., Sempéré, R., 2019. Macro-litter in surface waters from the Rhone River: Plastic pollution and loading to the NW Mediterranean Sea. Marine Pollution Bulletin 146, 60–66. https://doi.org/10.1016/j.marpolbul.2019.05.067

Cheung, P.K., Cheung, L.T.O., Fok, L., 2016. Seasonal variation in the abundance of marine plastic debris in the estuary of a subtropical macro-scale drainage basin in South China. Science of The Total Environment 562, 658–665. https://doi.org/10.1016/j.scitotenv.2016.04.048

Cordeiro, C.A.M.M., Costa, T.M., 2010. Evaluation of solid residues removed from a mangrove swamp in the São Vicente Estuary, SP, Brazil. Marine Pollution Bulletin 60, 1762–1767. https://doi.org/10.1016/j.marpolbul.2010.06.010

Dris, R., Tramoy, R., Alligant, S., Gasperi, J., Tassin, B., 2020. Plastic Debris Flowing from Rivers to Oceans: The Role of the Estuaries as a Complex and Poorly Understood Key Interface, in: Rocha-Santos, T., Costa, M., Mouneyrac, C. (Eds.), Handbook of Microplastics in the Environment. Springer International Publishing, Cham, pp. 1–28. https://doi.org/10.1007/978-3-030-10618-8_3-1

Duncan, E.M., Davies, A., Brooks, A., Chowdhury, G.W., Godley, B.J., Jambeck, J., Maddalene, T., Napper, I., Nelms, S.E., Rackstraw, C., Koldewey, H., 2020. Message in a bottle: Open source technology to track the movement of plastic pollution. PLoS ONE 15, e0242459. https://doi.org/10.1371/journal.pone.0242459

GIP, 2014. Les mouvements. Les sédiments. La dynamique du bouchon vaseux. Cahier indicateur du GIP Loire Estuaire 1.

GIP, 2016. Inventaire des roselières de l'estuaire de la Loire, acquisition et analyse de données. Précisions méthodologiques et analyse diachronique. Rapport du GIP Loire Estuaire.

Gonçalves, M., Schmid, K., Andrade, M.C., Andrades, R., Pegado, T., Giarrizzo, T., 2020. Are the tidal flooded forests sinks for litter in the Amazonian estuary? Marine Pollution Bulletin 161, 111732. https://doi.org/10.1016/j.marpolbul.2020.111732

González-Fernández, D., Cózar, A., Hanke, G., Viejo, J., Morales-Caselles, C., Bakiu, R., Barceló, D., Bessa, F., Bruge, A., Cabrera, M., Castro-Jiménez, J., Constant, M., Crosti, R., Galletti, Y., Kideys, A.E., Machitadze, N., Pereira de Brito, J., Pogojeva, M., Ratola, N., Rigueira, J., Rojo-Nieto, E., Savenko, O., Schöneich-Argent, R.I., Siedlewicz, G., Suaria, G., Tourgeli, M., 2021. Floating macrolitter leaked from Europe into the ocean. Nature Sustainability 4, 474–483. https://doi.org/10.1038/s41893-021-00722-6

Hajbane, S., Pattiaratchi, C.B., 2017. Plastic Pollution Patterns in Offshore, Nearshore and Estuarine Waters: A Case Study from Perth, Western Australia. Frontiers in Marine Science 4. https://doi.org/10.3389/fmars.2017.00063

Ivar do Sul, J.A., Costa, M.F., 2013. Plastic pollution risks in an estuarine conservation unit. Journal of Coastal Research 65, 48–53. https://doi.org/10.2112/SI65-009.1

Ivar do Sul, J.A., Costa, M.F., Silva-Cavalcanti, J.S., Araújo, M.C.B., 2014. Plastic debris retention and exportation by a mangrove forest patch. Marine Pollution Bulletin 78, 252–257. https://doi.org/10.1016/j.marpolbul.2013.11.011

Kassambara, A., Mundt, F., 2020. Factoextra: Extract and Visualize the Results of Multivariate Data Analyses. R Package Version 1.0.7. https://CRAN.R-project.org/package=factoextra

Krelling, A.P., Turra, A., 2019. Influence of oceanographic and meteorological events on the quantity and quality of marine debris along an estuarine gradient. Marine Pollution Bulletin 139, 282–298. https://doi.org/10.1016/j.marpolbul.2018.12.049

Kurniawan, S.B., Imron, M.F., 2019a. The effect of tidal fluctuation on the accumulation of plastic debris in the Wonorejo River Estuary, Surabaya, Indonesia. Environmental Technology & Innovation 15, 100420. https://doi.org/10.1016/j.eti.2019.100420

Kurniawan, S.B., Imron, M.F., 2019b. Seasonal variation of plastic debris accumulation in the estuary of Wonorejo River, Surabaya, Indonesia. Environmental Technology & Innovation 16, 100490. https://doi.org/10.1016/j.eti.2019.100490

Lê, S., Josse, J., Husson, F., 2008. FactoMineR: An R Package for Multivariate Analysis. Journal of Statistical Software 25. https://doi.org/10.18637/jss.v025.i01

Lechthaler, S., Waldschläger, K., Stauch, G., Schüttrumpf, H., 2020. The Way of Macroplastic through the Environment. Environments 7, 73. https://doi.org/10.3390/environments7100073

Liro, M., Emmerik, T. van, Wyżga, B., Liro, J., Mikuś, P., 2020. Macroplastic Storage and Remobilization in Rivers. Water 12, 2055. https://doi.org/10.3390/w12072055

Liro, M., Mikuś, P., Wyżga, B., 2022. First insight into the macroplastic storage in a mountain river: The role of in-river vegetation cover, wood jams and channel morphology. Science of The Total Environment 838, 156354. https://doi.org/10.1016/j.scitotenv.2022.156354

Maclean, K., Weideman, E.A., Perold, V., Ryan, P.G., 2021. Buoyancy affects stranding rate and dispersal distance of floating litter entering the sea from river mouths. Marine Pollution Bulletin 173, 113028. https://doi.org/10.1016/j.marpolbul.2021.113028

Maximenko, N., Corradi, P., Law, K.L., Van Sebille, E., Garaba, S.P., Lampitt, R.S., Galgani, F., Martinez-Vicente, V., Goddijn-Murphy, L., Veiga, J.M., Thompson, R.C., Maes, C., Moller, D., Löscher, C.R., Addamo, A.M., Lamson, M.R., Centurioni, L.R., Posth, N.R., Lumpkin, R., Vinci, M., Martins, A.M., Pieper, C.D., Isobe, A., Hanke, G., Edwards, M., Chubarenko, I.P., Rodriguez, E., Aliani, S., Arias, M., Asner, G.P., Brosich, A., Carlton, J.T., Chao, Y., Cook, A.-M., Cundy, A.B., Galloway, T.S., Giorgetti, A., Goni, G.J., Guichoux, Y., Haram, L.E., Hardesty, B.D., Holdsworth, N., Lebreton, L., Leslie, H.A., Macadam-Somer, I., Mace, T., Manuel, M., Marsh, R., Martinez, E., Mayor, D.J., Le Moigne, M., Molina Jack, M.E., Mowlem, M.C., Obbard, R.W., Pabortsava, K., Robberson, B., Rotaru, A.-E., Ruiz, G.M., Spedicato, M.T., Thiel, M., Turra, A., Wilcox, C., 2019. Toward the Integrated Marine Debris Observing System. Frontiers in Marine Science 6, 447. https://doi.org/10.3389/fmars.2019.00447

Mazarrasa, I., Puente, A., Núñez, P., García, A., Abascal, A.J., Juanes, J.A., 2019. Assessing the risk of marine litter accumulation in estuarine habitats. Marine Pollution Bulletin 144, 117–128. https://doi.org/10.1016/j.marpolbul.2019.04.060

Meijer, L.J.J., van Emmerik, T., van der Ent, R., Schmidt, C., Lebreton, L., 2021. More than 1000 rivers account for 80% of global riverine plastic emissions into the ocean. Science Advances 7, eaaz5803. https://doi.org/10.1126/sciadv.aaz5803

Pinheiro, L.M., Agostini, V.O., Lima, A.R.A., Ward, R.D., Pinho, G.L.L., 2021. The fate of plastic litter within estuarine compartments: An overview of current knowledge for the transboundary issue to guide future assessments. Environmental Pollution 279, 116908. https://doi.org/10.1016/j.envpol.2021.116908

Possatto, F.E., Spach, H.L., Cattani, A.P., Lamour, M.R., Santos, L.O., Cordeiro, N.M.A., Broadhurst, M.K., 2015. Marine debris in a World Heritage Listed Brazilian estuary. Marine Pollution Bulletin 91, 548–553. https://doi.org/10.1016/j.marpolbul.2014.09.032

QGIS.org, 2022. QGIS Geographic Information System. QGIS Association. http://www.qgis.org

Rech, S., Macaya-Caquilpán, V., Pantoja, J.F., Rivadeneira, M.M., Jofre Madariaga, D., Thiel, M., 2014. Rivers as a source of marine litter – A study from the SE Pacific. Marine Pollution Bulletin 82, 66–75. https://doi.org/10.1016/j.marpolbul.2014.03.019

RStudio Team, 2021. RStudio: Integrated Development Environment for R. RStudio, PBC, Boston, MA. http://www.rstudio.com/

Ryan, P.G., Perold, V., 2021. Limited dispersal of riverine litter onto nearby beaches during rainfall events. Estuarine, Coastal and Shelf Science 251, 107186. https://doi.org/10.1016/j.ecss.2021.107186

Sadri, S.S., Thompson, R.C., 2014. On the quantity and composition of floating plastic debris entering and leaving the Tamar Estuary, Southwest England. Marine Pollution Bulletin 81, 55–60. https://doi.org/10.1016/j.marpolbul.2014.02.020

SAGE, 2020. Plan d'aménagement et de gestion durable de la ressource en eau. Rapport du Schéma d'aménagement et de gestion des eaux, Estuaire de la Loire.

Schmidt, C., Krauth, T., Wagner, S., 2017. Export of Plastic Debris by Rivers into the Sea. Environmental Science & Technology 51, 12246–12253. https://doi.org/10.1021/acs.est.7b02368

Schöneich-Argent, R.I., Dau, K., Freund, H., 2020. Wasting the North Sea? – A field-based assessment of anthropogenic macrolitter loads and emission rates of three German tributaries. Environmental Pollution 263, 114367. https://doi.org/10.1016/j.envpol.2020.114367

Sellier, D., 2012. Géomorphologie de l'estuaire de la Loire, éléments de vulgarisation et de patrimonialisation. Cahiers Nantais d'Aménagement 1, 45–64.

SNPN, 2008. Estuaires, deltas et baies. Rapport de la Société nationale de protection de la nature. Zones Humides Infos 61, 32.

Tramoy, R., Gasperi, J., Colasse, L., Tassin, B., 2020a. Transfer dynamic of macroplastics in estuaries — New insights from the Seine estuary: Part 1. Long term dynamic based on date-prints on stranded debris. Marine Pollution Bulletin 152, 110894. https://doi.org/10.1016/j.marpolbul.2020.110894

Tramoy, R., Gasperi, J., Colasse, L., Silvestre, M., Dubois, P., Noûs, C., Tassin, B., 2020b. Transfer dynamics of macroplastics in estuaries – New insights from the Seine estuary: Part 2. Short-term dynamics based on GPS-trackers. Marine Pollution Bulletin 160, 111566. https://doi.org/10.1016/j.marpolbul.2020.111566

Tramoy, R., Gasperi, J., Colasse, L., Noûs, C., Tassin, B., 2021. Transfer dynamics of macroplastics in estuaries – New insights from the Seine estuary: Part 3. What fate for macroplastics? Marine Pollution Bulletin 169, 112513. https://doi.org/10.1016/j.marpolbul.2021.112513

van Calcar, C.J., van Emmerik, T.H.M., 2019. Abundance of plastic debris across European and Asian rivers. Environmental Research Letters 14, 124051. https://doi.org/10.1088/1748-9326/ab5468

van Emmerik, T., Strady, E., Kieu-Le, T.-C., Nguyen, L., Gratiot, N., 2019. Seasonality of riverine macroplastic transport. Sci Rep 9, 13549. https://doi.org/10.1038/s41598-019-50096-1

van Emmerik, T., Schwarz, A., 2020. Plastic debris in rivers. WIREs Water 7, e1398. https://doi.org/10.1002/wat2.1398

van Emmerik, T., Roebroek, C., de Winter, W., Vriend, P., Boonstra, M., Hougee, M., 2020a. Riverbank macrolitter in the Dutch Rhine–Meuse delta. Environmental Research Letters 15, 104087. https://doi.org/10.1088/1748-9326/abb2c6

van Emmerik, T., van Klaveren, J., Meijer, L.J.J., Krooshof, J.W., Palmos, D.A.A., Tanchuling, M.A., 2020b. Manila River Mouths Act as Temporary Sinks for Macroplastic Pollution. Frontiers in Marine Science 7, 545812. https://doi.org/10.3389/fmars.2020.545812

van Emmerik, T., Mellink, Y., Hauk, R., Waldschläger, K., Schreyers, L., 2022. Rivers as Plastic Reservoirs. Frontiers in Water 3, 786936. https://doi.org/10.3389/frwa.2021.786936

Vegter, A., Barletta, M., Beck, C., Borrero, J., Burton, H., Campbell, M., Costa, M., Eriksen, M., Eriksson, C., Estrades, A., Gilardi, K., Hardesty, B., Ivar do Sul, J., Lavers, J., Lazar, B., Lebreton, L., Nichols, W., Ribic, C., Ryan, P., Schuyler, Q., Smith, S., Takada, H., Townsend, K., Wabnitz, C., Wilcox, C., Young, L., Hamann, M., 2014. Global research priorities to mitigate plastic pollution impacts on marine wildlife. Endangered Species Research 25, 225–247. https://doi.org/10.3354/esr00623

Vermeiren, P., Muñoz, C.C., Ikejima, K., 2016. Sources and sinks of plastic debris in estuaries: A conceptual model integrating biological, physical and chemical distribution mechanisms. Marine Pollution Bulletin 113, 7–16. https://doi.org/10.1016/j.marpolbul.2016.10.002

Weideman, E.A., Perold, V., Arnold, G., Ryan, P.G., 2020. Quantifying changes in litter loads in urban stormwater run-off from Cape Town, South Africa, over the last two decades. Science of The Total Environment 724, 138310. https://doi.org/10.1016/j.scitotenv.2020.138310

Wickham, H., 2016. ggplot2: Elegant Graphics for Data Analysis. Springer-Verlag New York. https://ggplot2.tidyverse.org

Williams, A.T., Simmons, S.L., 1997. Movement patterns of riverine litter. Water, Air, and Soil Pollution 98, 119–139. https://doi.org/10.1007/BF02128653

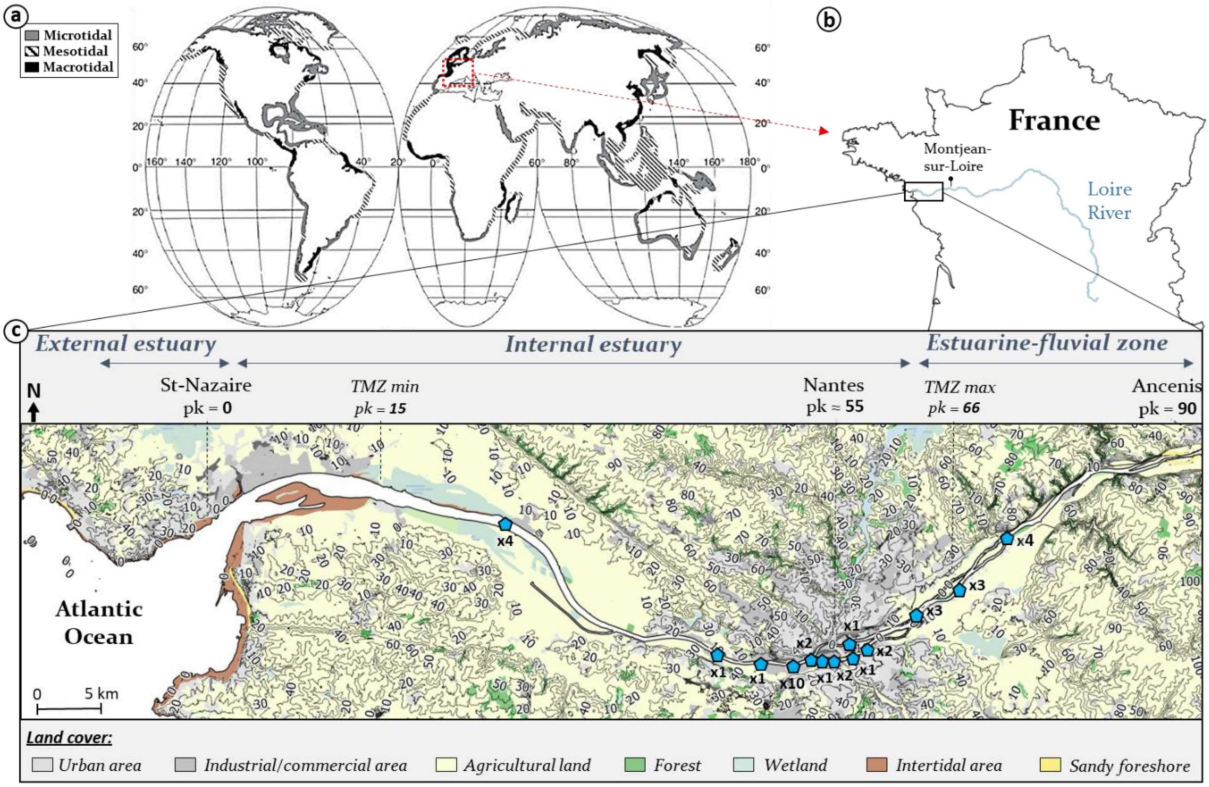

Figure 1: a) World map of the types of estuaries (www.aquaportail.com) and position of France, b) map of France and of the Loire estuary, c) map of the Loire estuary with the tracked bottles sites of release (blue pentagons). The number of tracked bottles released is indicated. The kilometric point (pk) 0 is set in St-Nazaire, pk are positively increasing upstream and negative downstream. From up to downstream, the tracked bottles were released in Mauves-sur-Loire (pk 72.2, Mid-bridge), St-Julien-de-Concelles (pk 66.9, Mid-bridge), Basse-Goulaine (pk 62.2, Mid-bridge), St-Sebastien-sur-Loire (pk 57.1, Mid-bridge), Nantes (pk 56.3 & 55.8, Mid-bridge; pk 50.7, 50.2, 50.1 & 50, Riverbanks), Rezé (pk 54.3, Mid-bridge; pk 53.5 & 52.4, Riverbanks), Bouguenais (pk 47.9 & 46.2, Riverbanks) and le Pellerin (pk 24.5, Riverbanks). The land cover (Corine Land Cover 2018 from www.data.gouv.fr), the topography, and the minimum and maximum positions of the Turbidity Maximum Zone (TMZ) are indicated.

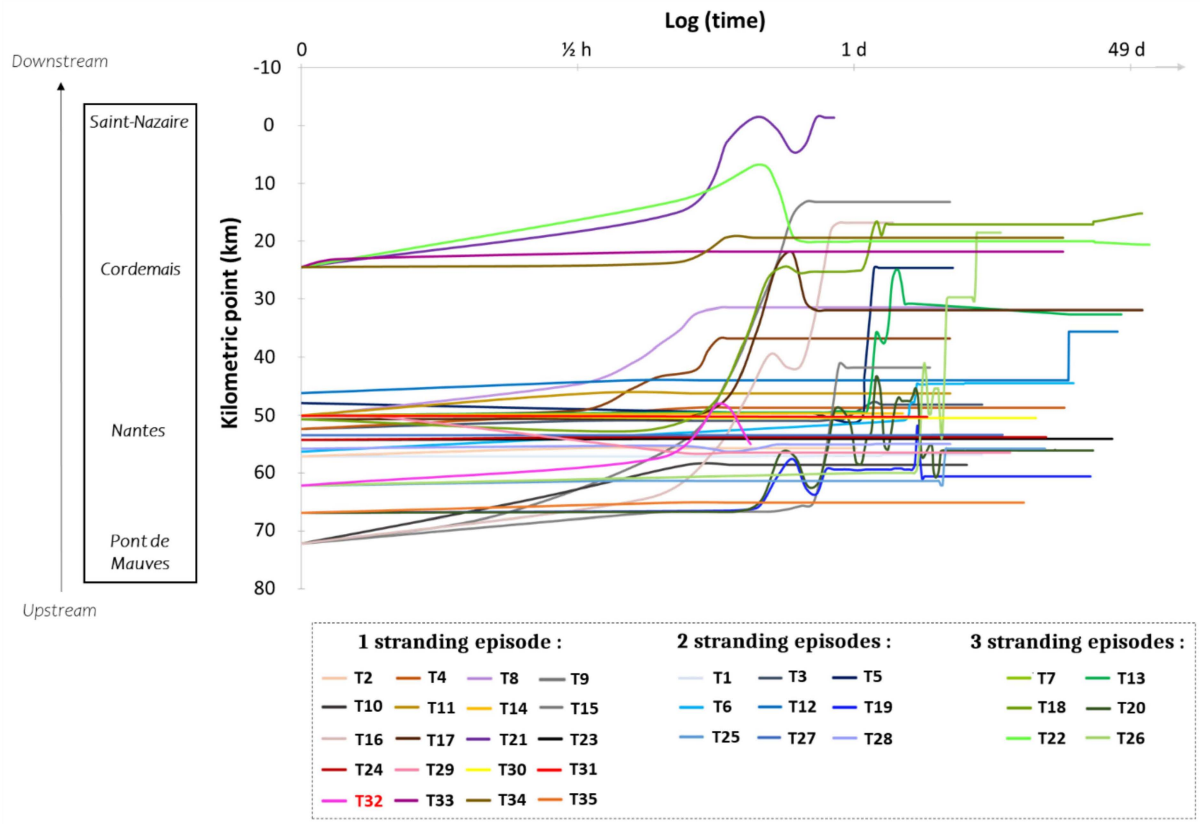

Figure 2: Kilometric point (pk in km) of the tracked bottles according to time (in hours noted h and days noted d) in a logarithmic scale. Colors of the trajectories were set according to the number of stranding episodes: random colors for 1 stranding episode (T32 appears in red since because of the loss of the signal no stranding episode was actually monitored), blue shades for 2 stranding episodes and green shades for 3 stranding episodes.

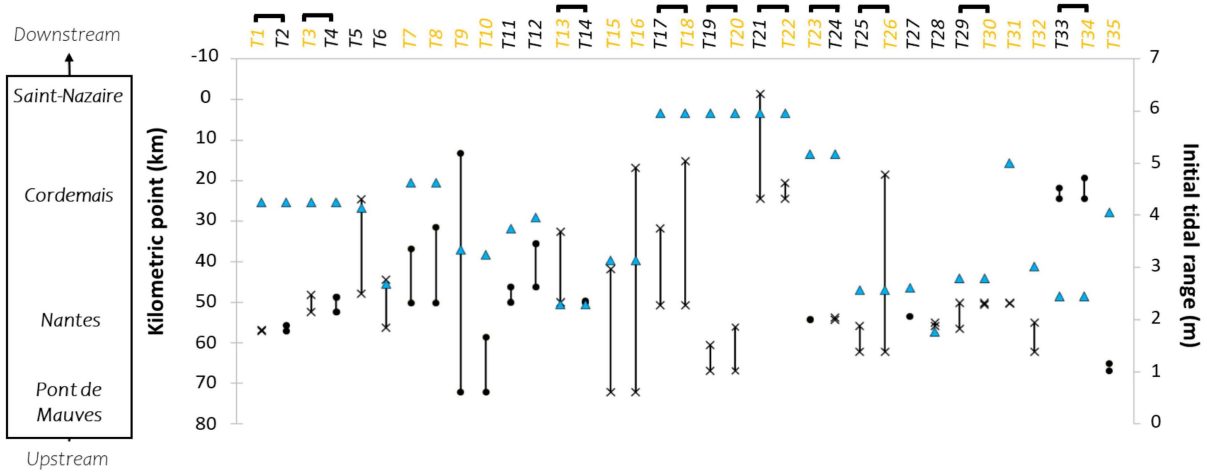

Figure 3: Net distances (in km) travelled by the tracked bottles from the initial to the final kilometric point (pk) according to the initial tidal range (blue triangles, in m). The trajectories for which a difference between total and net distances was observed are represented by crosses at initial and final points. Trajectories of floating bottles are named in black, trajectories of half-submerged bottles are named in yellow and paired bottles are indicated by brackets.

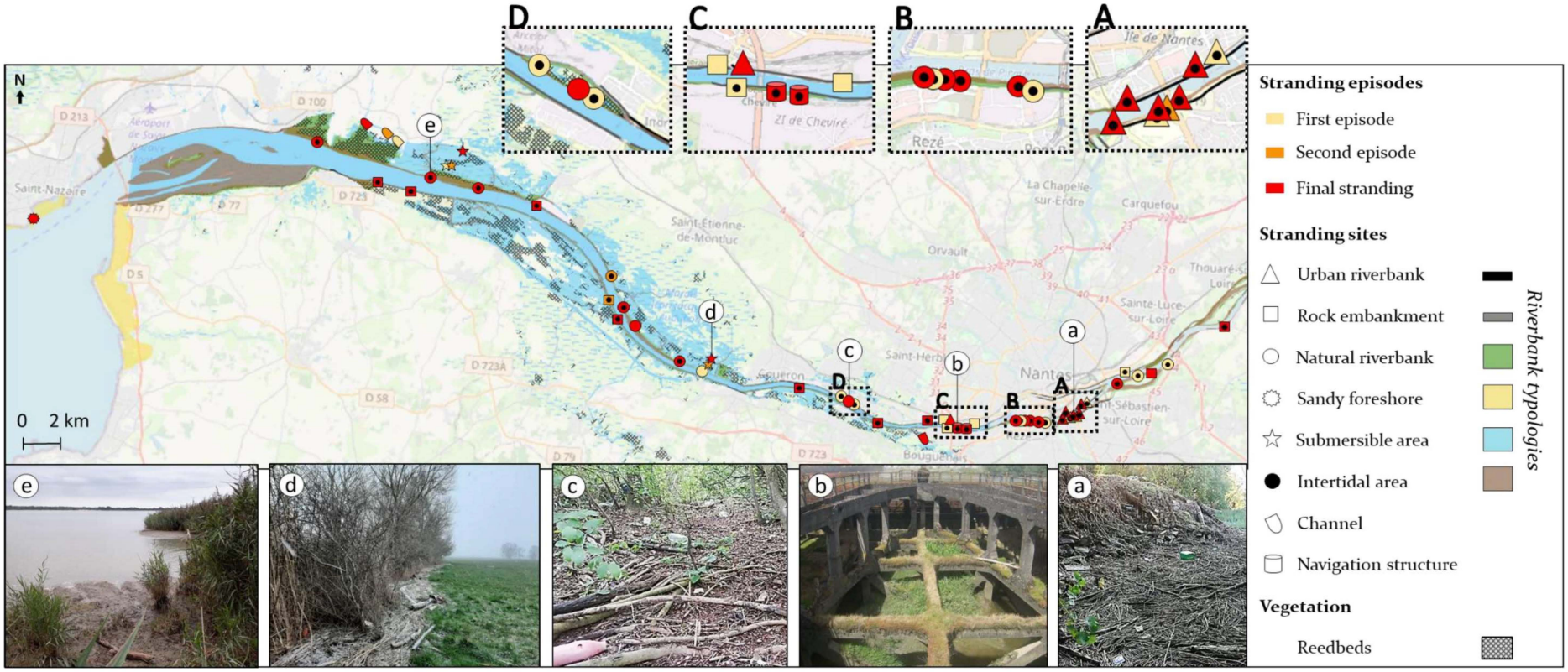

614

615 *Figure 4: Map of the stranding conditions of the tracked bottles with colors corresponding to their potential remobilization and symbols corresponding to the stranding sites.*
616 *The riverbank typologies and the presence of reedbeds (data from the GIP Loire Estuaire) in the Loire estuary are represented as well as photos of some accumulation zones*
617 *(a: at fixed urban riverbanks south of Nantes Métropole, b:in harbor structures, c: at the la Motte island, d: at riparian vegetation of submersible areas, e: in reedbeds).*

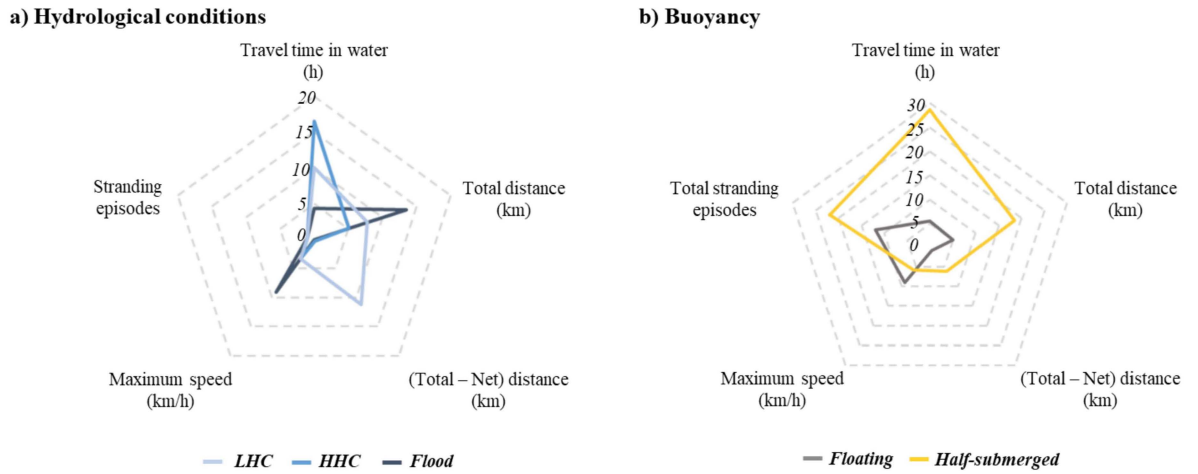

Figure 5: a) Median values of different parameters according to hydrological conditions (Low hydrological conditions, n(LHC) = 17; High hydrological conditions, n(HHC) = 12; and n(Flood) = 6). b) Median values of travel time in water (in hours noted h), total distance and (Total – Net) distance (in km), maximum values of speeds (in km/h) and total number of stranding episodes according to bottles buoyancy (floating, n = 10; and half-submerged, n = 10).

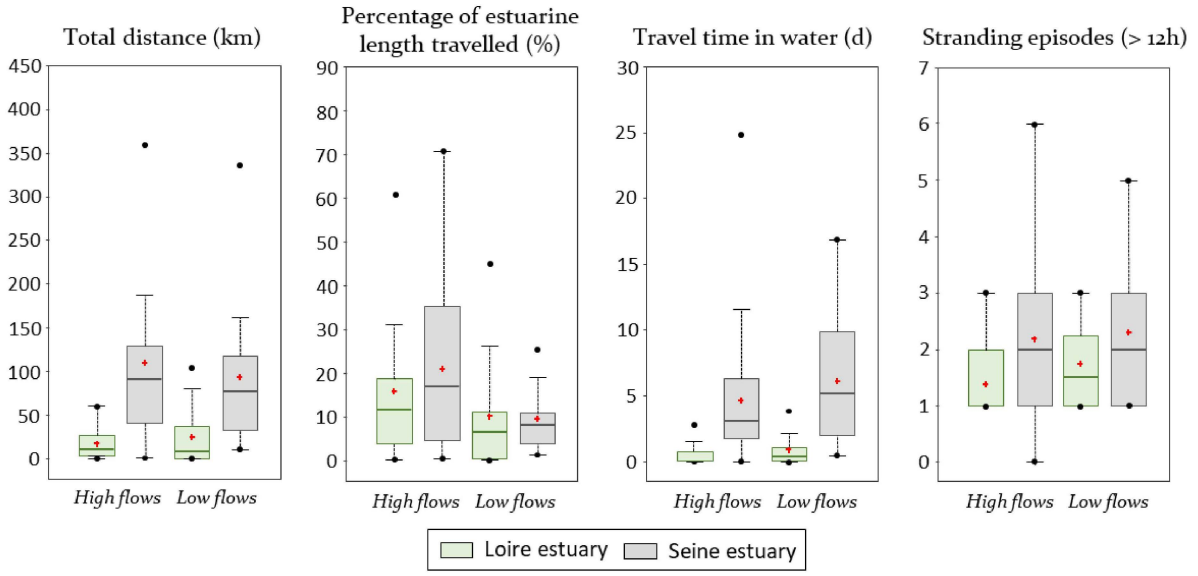

Figure 6: Boxplots representing the variability (first quartile, third quartile and median; red crosses: mean values; vertical bars: 1.5 time the interquartile range) of the total distance (in km), the percentages of estuarine length travelled by the bottles (calculated by dividing the net distance by the total length of estuary), the travel time in water (in days noted d) and the number of stranding episodes according to the estuary considering the hydrological conditions: high (n(Loire) = 18; and n(Seine) = 23) and low flows (n(Loire) = 17; and n(Seine) = 13).

Table 1: Parameters describing initial and final conditions, durations, distances, speeds and stranding/remobilization conditions of the trajectories in the Loire River. Parameters reporting hydrometeorological conditions are also included. All the results of these parameters are reported in the supplementary materials. Black stars indicate the common parameters with the study in the Seine estuary (Tramoy et al., 2020b).

Initial conditions		
*Start time**	Day and time of release	Date, hour
*Site of release**	Geographical site where the tracked bottle was released	-
*Start pk**	Kilometric point (pk) of the site of release	Km
*Buoyancy**	Buoyancy of the tracked bottle (e.g. floating or half-submerged)	-
Final conditions		
*End time**	Day and time of the last GPS position recorded	Date, hour
*Last stranding**	Day and time of the last stranding before loss of signal or bottle retrieve	Date, hour
*End site**	Geographical site where the tracked bottle was retrieved or lost	-
*End pk**	Kilometric point (pk) of the end site	Km
Durations		
Total duration	Time between end time and start time including periods of stranding (> 12h)	Day
*Travel Time**	Time between last stranding and start time including periods of stranding (> 12h)	Day
*Travel Time in water**	Time between last stranding and start time without periods of stranding (> 12h)	Day
*Stranding Time**	Cumulative time of stranding (> 12h) until last stranding	Day
Distances		
*Total distance**	Cumulative distance between absolute values of pk of each GPS position	Km
*Net distance**	Net distance travelled by the tracked bottles	Km

(Total - Net) distances	Difference between total and net distances travelled by the tracked bottles	Km
Speeds		
Maximum speed	Maximum speed reached by the tracked bottles during their travel time in water	Km/h
Stranding/remobilization conditions		
*Stranding episodes (> 12h)**	Number of stranding episodes greater than a complete tidal cycle	-
Remobilization episodes	Number of remobilization episodes	-
Date of stranding	Day and time of stranding	Date, hour
Date of remobilization	Day and time of remobilization	Date, hour
River side	Side of the river where the tracked bottles is stranded and/or remobilized (north, south or island)	-
Riverbank and vegetation typologies	Characteristics of the stranding and/or remobilization site	-
Tidal and hydrometeorological conditions		
*Water flow**	Water flow at start time (Q_i, in Montjean-sur-Loire, http://www.hydro.eaufrance.fr/)	m^3/s
Water level	Water levels at start time and at stranding (in St-Nazaire, http://maree.info/)	m
Flood or ebb tides	Flood or ebb tides at stranding (in St-Nazaire, http://maree.info/)	-
Tidal ranges	Tidal ranges at start time and at strandings (in St-Nazaire, http://maree.info/)	m